

New Family of Ruddlesden–Popper Strontium Niobium Oxynitrides: $(\text{SrO})(\text{SrNbO}_{2-x}\text{N})_n$ ($n = 1, 2$)Gerard Tobías, Judith Oró-Solé, D. Beltrán-Porter,[†] and Amparo Fuertes*

Institut de Ciència de Materials de Barcelona (CSIC), Campus UAB, 08193 Bellaterra, Spain, and Institut de Ciència de Materials de la Universitat de València, P.O. BOX 2085, Polígono “La Coma” s/n, 46980 Paterna, Spain

Received July 26, 2001

New superconducting compounds containing transition metals other than copper have been a constant goal for chemists since the discovery of superconductivity in cuprates.¹ One of the most explored classes of compounds within this trend has been the layered oxides from early transition metals, with special emphasis on those showing electron configurations complementary to Cu(II)/Cu(III) or Cu(II)/Cu(I), that is, d^1/d^2 or d^1/d^0 systems. Examples of success following this approach are the superconductors Li_2NbO_2 ² and $\text{KCa}_2\text{Nb}_3\text{O}_{10}$.³ In the field of nitrides, superconductivity has been recently reported for mixed valence d^0/d^1 zirconium and hafnium nitride halides, showing some of the highest critical temperatures for non-oxide systems.^{4,5,6} Niobium and tantalum oxynitrides with perovskite structure were first reported by Marchand et al.⁷ and recently have attracted interest because of their potential use as nontoxic inorganic pigments.⁸ Strontium tantalum oxynitride $\text{Sr}_2\text{TaO}_3\text{N}$ ⁹ shows the K_2NiF_4 structure and is the first example of a Ruddlesden–Popper phase containing only tantalum and an alkaline earth metal as constituent cations. Ternary alkaline earth Ruddlesden–Popper oxides from group IV of the transition metals are known only for titanium, forming the family of compounds $\text{A}_{n+1}\text{Ti}_n\text{O}_{3n+1}$.¹⁰ As the +4 oxidation state is less stable in air for Nb and Ta than for Ti, these metals adopt other structural types allowing the +5 oxidation state when combined with alkaline earth metals. The electronic configurations for the possible oxidation states for Nb (+5, +4, +3), as well as its ability to form mixed-valence compounds, make this element a good candidate for the search for new layered compounds with electronic conductivity or superconductivity. In this paper, we present the synthesis and structural characterization of two members of the new family $(\text{SrO})(\text{SrNbO}_{2-x}\text{N})_n$ ($n = 1, 2$). These compounds, with formulas $\text{Sr}_2\text{NbO}_{3-x}\text{N}$ ($n = 1$) and $\text{Sr}_3\text{Nb}_2\text{O}_{5-x}\text{N}_2$ ($n = 2$), constitute the first strontium niobium Ruddlesden–Popper oxynitrides and provide layered parent structures, analogous to La_2CuO_4 ,¹ Sr_2RuO_4 ,¹¹ and $\text{La}_2\text{CaCu}_2\text{O}_6$,¹² to obtain mixed valence niobium compounds with a variety of oxidation states and transport properties.

Samples with composition $\text{Sr}_2\text{NbO}_x\text{N}_y$ ($n = 1$) and $\text{Sr}_3\text{Nb}_2\text{O}_x\text{N}_y$ ($n = 2$) were prepared by solid-state reaction of SrCO_3 (Baker, 99.9%) and Nb_2O_5 (Aldrich, 99.99%), with molar ratios 4:1 for

* Author to whom correspondence should be addressed. E-mail: amparo.fuertes@icmab.es.

[†] Institut de Ciència de Materials de la Universitat de València.

- (1) Bednorz, J. G.; Müller, K. A. *Z. Phys. B: Condens. Matter* **1986**, *64*, 189.
- (2) Geselbracht, M. J.; Richardson, T. J.; Stacy, A. M. *Nature* **1990**, *345*, 324.
- (3) Takano, Y.; Takayanagi, S.; Ogawa, S.; Yamada, T.; Mōri, N. *Solid State Commun.* **1997**, *103*, 215.
- (4) Yamanaka, S.; Hohetama, K.; Kawaji, H. *Nature* **1998**, *392*, 580.
- (5) Fuertes, A.; Vlassov, M.; Beltrán-Porter, D.; Alemany, P.; Canadell, E.; Casañ-Pastor, N.; Palacín, M. R. *Chem. Mater.* **1999**, *11*, 203.
- (6) Yamanaka, S. *Annu. Rev. Mater. Sci.* **2000**, *30*, 53.
- (7) Marchand, R.; Pors, F.; Laurent, Y. *Rev. Int. Hautes Tempér. Réfract.* **1986**, *23*, 11.
- (8) Jansen, M.; Letschert, H. P. *Nature* **2000**, *404*, 980.
- (9) Diot, N.; Marchand, R.; Haines, J.; Léger, J. M.; Macaudière, P.; Hull, S. J. *Solid State Chem.* **1999**, *146*, 390.
- (10) Ruddlesden, S. N.; Popper, P. *Acta Crystallogr.* **1957**, *10*, 538; **1958**, *11*, 54.

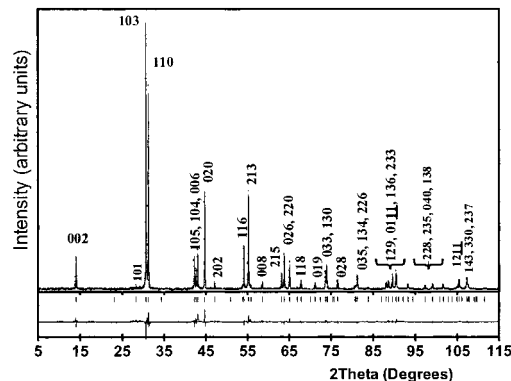


Figure 1. Observed and calculated X-ray diffraction patterns for $\text{Sr}_2\text{NbO}_{2.8}\text{N}$.

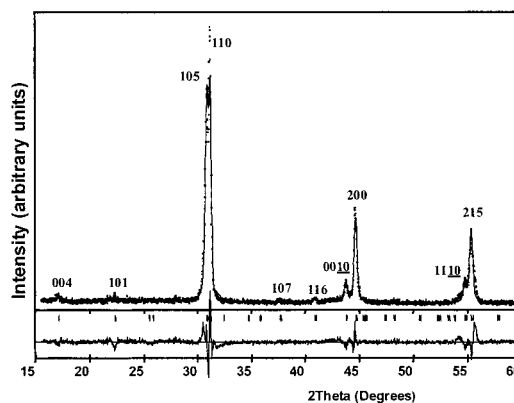


Figure 2. X-ray diffraction pattern for $\text{Sr}_3\text{Nb}_2\text{O}_{4.7}\text{N}_2$.

$n = 1$ and 3:1 for $n = 2$. The reactants were pelletized and treated under flowing NH_3 ($180 \text{ cm}^3/\text{min}$) (Carburros Metálicos, 99.9%) at temperatures between 900 and 1050 °C for several 50 h cycles with intermediate regrinding. Samples were air-sensitive, and their handling between thermal cycles as for subsequent characterization was done in an Ar-filled glovebox. The final color of both samples was dark brown, which gradually changed to light brown on air exposure. X-ray diffraction patterns were generally taken in a Rigaku Rotaflex RU-200B rotating anode diffractometer using $\text{Cu K}\alpha$ radiation and, in some cases, protecting the samples with a Kapton film. Powder X-ray diffraction data collection for the crystal structure determination of $\text{Sr}_2\text{NbO}_{2.8}\text{N}$ was performed on an INEL curved position sensitive CPS120 powder diffractometer in a horizontal Debye–Scherrer geometry using a rotating capillary of diameter 0.1 mm as sample holder. The angular range was 120°, and the radiation was $\text{Cu K}\alpha 1$ ($\lambda = 1.540598 \text{ \AA}$), obtained with a Ge (111) monochromator. The sample was sieved

(11) Maeno, Y.; Hashimoto, H.; Yoshida, K.; Nishizaki, S.; Fujita, T.; Bednorz, J. G.; Lichtenberg, F. *Nature* **1994**, *372*, 532.

(12) Fuertes, A.; Obradors, X.; Navarro, J. M.; Gómez-Romero, P.; Casañ-Pastor, N.; Pérez, F.; Fontcuberta, J.; Miravittles, C.; Rodríguez-Carvajal, J.; Martínez, B. *Physica C* **1990**, *170*, 153.

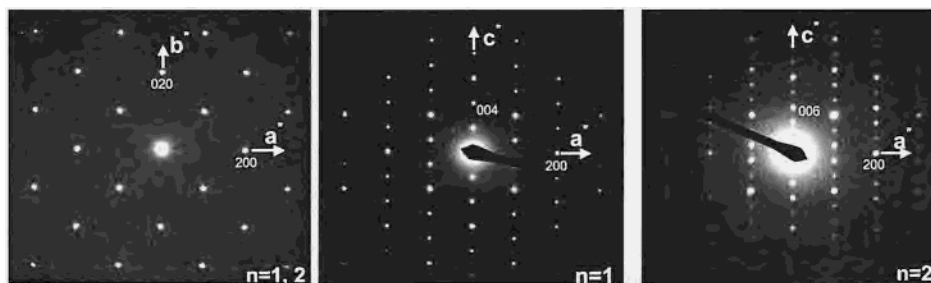


Figure 3. Electron diffraction patterns along [001] and [010] zone axes for (SrO)(SrNbO_{2-x}N)_n ($n = 1, 2$).

Table 1. Crystallographic Parameters for Sr₂NbO_{2.8}N (Space Group *I4/mmm*, $Z = 2$, $a = 4.0491(2)$ Å, $c = 12.5955(6)$ Å)

| | site | x/a | y/b | z/c | occ | B |
|---|------|-------|-------|--------------|-----|---------|
| Sr | 4e | 0 | 0 | 0.353 94(11) | 1 | 1.90(6) |
| Nb | 2a | 0 | 0 | 0 | 1 | 1.91(5) |
| N(1) | 4c | 0 | 0.5 | 0 | 0.5 | 0.9(2) |
| O(1) | 4c | 0 | 0.5 | 0 | 0.4 | 0.9(2) |
| O(2) | 4e | 0 | 0 | 0.1596(8) | 1 | 2.8(3) |
| $d(\text{Nb}-\text{N}, \text{O}(1)) (\times 4)$ (Å) | | | | | | |
| 2.025(1) | | | | | | |
| $d(\text{Nb}-\text{O}(2)) (\times 2)$ (Å) | | | | | | |
| 2.015(1) | | | | | | |
| $d(\text{Sr}-\text{O}, \text{N}(1))$ (Å) ($\times 4$) | | | | | | |
| 2.736(1) | | | | | | |
| $d(\text{Sr}-\text{O}(2))$ (Å) | | | | | | |
| 2.442(1) | | | | | | |
| $d(\text{Sr}-\text{O}(2))$ (Å) ($\times 4$) | | | | | | |
| 2.868(1) | | | | | | |
| $N_p, N_{\text{ref}}, N_{\text{iref}}^a$ | | | | | | |
| 3457, 70, 60 | | | | | | |
| P_p, P_i, P_g | | | | | | |
| 13, 8, 7 | | | | | | |
| $R_{\text{Bragg}}, R_F, \chi^2$ | | | | | | |
| 5.69, 4.85, 13.0 | | | | | | |
| $R_p, R_{\text{wp}}, R_{\text{exp}}$ | | | | | | |
| 18.2, 23.6, 6.47 | | | | | | |
| f_p | | | | | | |
| 2.5 | | | | | | |

^a Conventional Rietveld R -factors (R_p, R_{exp}) are calculated by using background corrected counts. Thermal vibrations were restricted to be isotropic and fixed in the last steps of the refinement. $N_p, N_{\text{ref}}, N_{\text{iref}}$ refer to the number of experimental points, total reflections, and independent reflections, respectively. P_p, P_i, P_g refer to the number of profile, intensity-dependent, and global refined parameters, respectively. The profile fitting of the data was performed with a pseudo-Voigt function, including asymmetry and preferred orientation corrections. Preferred orientation and asymmetry were corrected, respectively, by the March–Dollase and the Berar–Bardinozzi expressions (see ref 13).

to 65 μm and mixed with glass powder before filling the capillary that was sealed under argon. The structure was solved by Rietveld analysis with the help of Fullprof.¹³ Electron diffraction patterns and XEDS analyses were obtained in a JEOL 1210 transmission electron microscope operating at 120 kV. Chemical compositions were determined by plasma absorption analyses (for cation contents), elemental analysis (for C and N contents), and TGA experiments performed in O₂ and Ar/H₂ (95/5, v/v). These lead to the compositions Sr₂NbO_{2.8}N and Sr₃Nb₂O_{4.7}N₂ for the $n = 1$ and $n = 2$ compounds, respectively. A reduced sample from the $n = 1$ phase was prepared by treating Sr₂NbO_{2.8}N at 447 °C in Ar/H₂.

Figures 1 and 2 show the X-ray diffraction patterns for Sr₂NbO_{2.8}N and Sr₃Nb₂O_{4.7}N₂.

In Figure 3, the electron diffraction patterns along the main crystallographic zone axes for the same phases are depicted. Indexation of the reflections in these planes and in others obtained by tilting around the three crystallographic axes lead to tetragonal unit cells with dimensions $a = 4.0$ Å and $c = 12.5$ Å for Sr₂NbO_{2.8}N, and $a = 4.0$ Å and $c = 20.7$ Å for Sr₃Nb₂O_{4.7}N₂. The observed reflection conditions in both compounds ($hkl, h + k + l = 2n; h00, h = 2n; 0k0, k = 2n; 00l, l = 2n; hk0, h + k = 2n; 0kl, k + l = 2n$, and $h0l, h + l = 2n$) were consistent with the space group *I4/mmm*. The starting coordinates for the structure determination of Sr₂NbO_{2.8} were taken from the compound Sr₂TaO₃N.⁹ Results for the best fitting are shown in Figure 1 and Table 1. For the $n = 2$ compound, the cell parameters, obtained from the pattern of Figure 2 with Fullprof but without introducing

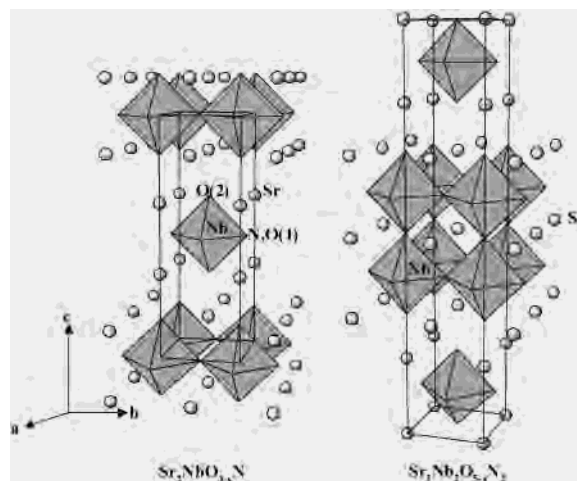


Figure 4. Perspective views of the structures of the $n = 1$ and $n = 2$ members of the family (SrO)(SrNbO_{2-x}N)_n.

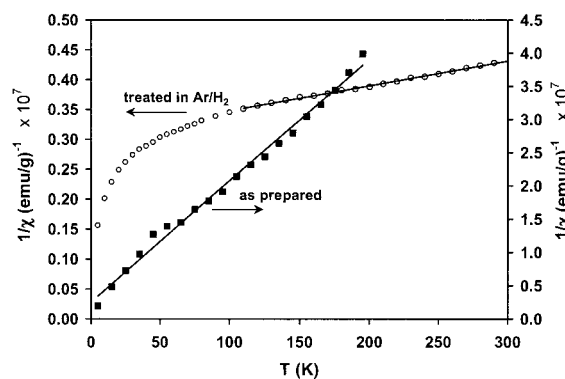


Figure 5. Magnetic susceptibility for as-prepared and reduced samples of Sr₂NbO_{2.8}N.

any structural model in the refinement, were $a = 4.0511(7)$ and $c = 20.651(9)$ Å. Perspective views of the structures for both compounds are shown in Figure 4.

The X-ray diffraction pattern and the electron diffraction micrographs of the $n = 2$ compound indicated a high degree of disorder in the stacking of planes perpendicular to the c direction. Thus, in this case, it is imperative to prepare new, better crystallized samples for the determination of accurate atom positions as well as to characterize fully the physical properties of this phase.

The N atoms in Sr₂NbO_{2.8}N were placed at the equatorial sites of the octahedron, site 1, taking the model found by Marchand et al. for Sr₂TaO₃N from neutron diffraction data.⁹ The bond distances in Table 1 are very close to those shown by the tantalum compound, in agreement with the identical ionic radii shown by Ta(V) and Nb(V) ($r(\text{CN} = 6) = 0.78$ Å).¹⁴ Occupation factors

(13) Rodríguez-Carvajal, J. *Program FULLPROF*, version 2.5; April 1994; ILL, unpublished.

for oxygen in sites 1 and 2 were refined, but the stoichiometry was fixed to 2.8 oxygen atoms per formula as found from N analysis and TGA oxidation experiments. The vacancies were found at the equatorial O(1) positions, although additional neutron diffraction experiments will be needed to confirm this result, as well as to determine the occupancies of nitrogen atoms in each site. The averaged formal oxidation state for niobium in this sample is +4.6. SQUID measurements (Figure 5) between room temperature and 4 K showed a paramagnetic behavior following a Curie–Weiss law with $\theta = -14$ K and $\mu_B = 0.11$ Bohr magnetons. The obtained μ_B is consistent with a +4/+5 mixed valence state for niobium. Magnetic measurements performed on one reduced sample (prepared by treatment in Ar/H₂ of the as-prepared sample), with a higher proportion of Nb(IV), showed the presence of strong antiferromagnetic interactions ($\theta = -733$ K) below 100 K, similar to those reported for layered cuprates¹⁵ (Figure 5). Electrical resistivity measurements performed on pellets sintered in NH₃ at 1000 °C of both as-prepared and reduced samples

showed that they are highly resistive. Further measurements, as well as doping or variation of N/O ratios in both $n = 1$ and $n = 2$ compounds will, however, be necessary to fully characterize the physical properties of the new compounds. The possibility of changing the anion stoichiometry as well as increasing the number of perovskite layers (n) will expand, indeed, the perspectives for finding new magnetic and transport properties in this family.

Acknowledgment. This study was supported by the MEC (Grant PB98-1424-C02) and the Comissionat per Universitats i Recerca de la Generalitat de Catalunya (Grant 2000SGR00113). G.T thanks FPI-MCYT for a fellowship. Dr. B. Martínez is acknowledged for his help in the measurement and interpretation of the magnetic and transport properties. The Serveis Científic Tècnics de l'Universitat de Barcelona and Pep Bassas are acknowledged for X-ray data acquisition of capillary samples.

IC0155661

(14) Shannon, R. D. *Acta Crystallogr. A* **1976**, *32*, 751.

(15) Johnston, D. C. *J. Magn. Mater.* **1991**, *100*, 218.